

Cannabinoid-2 Agonism with AM2301 Mitigates Morphine-Induced Respiratory Depression

Beth M. Wiese,¹ Erika Liktor-Busa,¹ Aidan Levine,¹ Sarah A. Couture,¹ Spyros P. Nikas,² Lipin Ji,² Yingpeng Liu,² Kenneth Mackie,³ Alexandros Makriyannis,² Tally M. Largent-Milnes,^{1,*†} and Todd W. Vanderah^{1,*†‡}

Abstract

Introduction: An escalating number of fatalities resulting from accidental opioid overdoses typically attributed to respiratory depression continue to define the opioid epidemic. Opioid respiratory depression results from a decrease in reflexive inspiration within the preBötzing complex in the brainstem.

Objective: Cannabinoid receptor agonism is reported to enhance opioid analgesia, yet whether cannabinoids enhance or inhibit opioid-induced respiratory depression is unknown.

Methods: Studies herein sought to define the roles of cannabinoid-1 receptor (CB1R) and cannabinoid-2 receptor (CB2R) on respiratory depression using selective agonists alone and in combination with morphine in male mice.

Results: Using whole body plethysmography, the nonselective CB1R and CB2R agonist (Δ^9 -tetrahydrocannabinol) and the CB1R synthetic cannabinoid, AM356, induced respiratory depression, whereas the well-published selective CB2 agonist, JWH 133, and the novel CB2 agonist (AM2301) did not. Moreover, a selective CB2R agonist (AM2301) significantly attenuated morphine sulfate-induced respiratory depression.

Conclusion: Notably, findings suggest that attenuation of opioid-induced respiratory depression relies on CB2R activation, supporting selective CB2R agonism as an opioid adjunct therapy.

Keywords: cannabinoid receptor 1; cannabinoid receptor 2; mu opioid receptor; opioid-induced respiratory depression; preBötzing complex

Introduction

Accidental overdose fatalities define the opioid epidemic despite alternative pain and opioid use disorder therapies.^{1,2} The U.S. Centers for Disease Control report 400,000 overdose deaths total with nearly 190 people dying daily.³ Respiratory depression is often the cause of death in opioid overdose that can be mitigated by opioid receptor antagonism with naloxone.⁴ Yet, adequate access and administration of naloxone to patients remains challenging.^{1,5,6} Therefore, identifying novel therapeutic strategies to prevent opioid-induced respiratory depression is vital.

Cannabinoids are analgesic in several models of pain^{5,7–11} and act synergistically with opioids,¹² allow-

ing for opioid sparing. Medicinal cannabis patients cite pain relief and opioid replacement as top reasons for use.¹³ Although cannabinoid-1 receptor (CB1R) activation induces pain relief and increases patient quality of life, agonists are associated with psychoactivity.¹⁴ In contrast, preclinical studies report that cannabinoid-2 receptor (CB2R) agonism reduces acute, chronic, and inflammatory pain without psychoactive side effects.^{8–11} However, the actions of cannabinoid compounds on respiration and interactions with opioid respiratory depression are unknown.

Studies here evaluated how cannabinoids influence respiratory function. Whole body plethysmography was performed after dosing with CB1R/CB2R agonists

¹Department of Pharmacology, University of Arizona, Tucson, Arizona, USA.

²Chemistry and Chemical Biology, Bouve College Health Sciences—Center for Drug Discovery, Northeastern University, Boston, Massachusetts, USA.

³Department of Psychological and Brain Sciences, Indiana University Bloomington, Bloomington, Indiana, USA.

Current affiliations: [†]Member of the Neuroscience GDP, University of Arizona, Tucson, Arizona, USA; [‡]Director of the Comprehensive Pain and Addiction Center, University of Arizona Health Sciences (UAHealth Sciences), Tucson, Arizona, USA.

*Address correspondence to: Tally M. Largent-Milnes, PhD, Department of Pharmacology, University of Arizona, 1501 North Campbell Avenue, Life Sciences North Room 621, Tucson, AZ 85724, USA, E-mail: tlargent@email.arizona.edu or Todd W. Vanderah, PhD, Department of Pharmacology, University of Arizona, 1501 North Campbell Avenue, Life Sciences North Room 621, Tucson, AZ 85724, USA, E-mail: vanderah@email.arizona.edu

alone and in combination with morphine sulfate (MS) suggested that activation of CB2R is sufficient to assuage MS-induced respiratory depression, whereas selective CB1R activation suppressed respiration.

Methods

Animals

Male CD1 mice (25–35 g) were obtained from Charles River Laboratories (Wilmington, MA) and housed in climate-controlled rooms on a 12-h light/dark cycle. Mouse pellet chow and water were available *ad libitum*. All procedures were approved and conform to the guidelines for the care and use of laboratory animals of the National Institutes of Health and were approved by the University of Arizona Animal Care and Use Committee.

Respiratory depression

Respiratory rates were measured in freely moving conscious mice using whole body plethysmography chambers (Data Sciences International, St. Paul, MN). Chambers were maintained at room temperature with flow and gas composition control. Vehicle (10% dimethyl sulfoxide [DMSO], 10% Tween-80, and 80% saline) or drug was administered intraperitoneally (i.p.) following a 30 min baseline. Mice remained in the chambers after injection for a 7-min room air (0% carbon dioxide/oxygen [CO₂]) condition, and a 7-min 5% concentration of CO₂ challenge.¹⁵

Primary outcome was respiratory rate (breaths per minute [BPM]) with secondary measures of minute ventilation and tidal volume. Data were normalized and presented as percentage of baseline to control for inter-animal variability. Groups are compared with same vehicle and morphine group throughout experiments.

Thermal antinociception

Tail withdrawal latency was assessed in uninjured animals. The distal two-thirds of the tail was placed in a 52°C circulating water bath and withdrawal latency was recorded (cutoff of 15 sec). After baseline, all mice were given an i.p. injection, and behavior was assessed at 15-, 30-, 45-, 60-, 90-, and 120-min postinjection. Mice were returned to their home cage between time points.

Model of postoperative pain

Anesthesia was induced with 5% isoflurane and maintained at 2.5% in 1.5 L/min of O₂. A 0.5-cm longitudinal incision was made through the skin and fascia on the plantar surface of the right hind paw.¹⁶ The plantaris muscle was elevated, separated from fascia, incised longitudinally, replaced, and closed with a 5–0 silk mattress suture.

Mechanical allodynia

Paw withdrawal thresholds were assessed using calibrated von Frey filaments applied to the planter surface of the incised paw. All mice were given an i.p. injection and behaviors were reassessed at 15, 30, 45, 60, 90, and 120 min. Mechanical allodynia was determined using the Chaplan up–down method.¹⁷

Tissue collection

Mice were anesthetized in an induction chamber with 5% isoflurane in 1.5 L/min of air. Mice were transcardially perfused (ice-cold phosphate-buffered saline). The spleen, periaqueductal gray (PAG; A/P –3.5 to –5), and preBötzing complex (pBc; A/P –6.84 to –7.08, M/L ±1.2–1.5 [Ref.¹⁸]) combined with inferior olive and closing of the fourth ventricle to ensure correct location, Supplementary Fig. S1A) were collected, immediately flash frozen in liquid nitrogen, and stored at –80°C.

Materials

Drugs and reagents

MS, a mu opioid receptor (MOR) agonist ($K_i=1.1$ nM¹⁹), was from the NIDA drug supply program (Rockville, MD). AM2301, a brain penetrant CB2R agonist (CB2 $K_i=1.3$ nM, CB1 $K_i=172$ nM), and AM356 (CB1R $K_i=37$ nM, CB2 $K_i > 1,000$ nM)^{20,21} were both gifts from Dr. Alexandros Makryiannis (Boston, MA). SR-144528, a CB2 inverse agonist (CB2 $K_i=0.6$ nM, CB1 $K_i=400$ nM),²² was from Sigma (St. Louis, MO). AM630, a CB2 inverse agonist (CB2 $K_i=32.1$ nM, CB1 $K_i=5152$ nM),²³ Δ^9 -tetrahydrocannabinol (THC), a mixed CB1R/CB2R agonist (CB1R $K_i=48$ nM, CB2R $K_i=40$ nM),^{24,25} and JWH 133, a selective CB2 agonist (CB2 $K_i=3.4$ nM, CB1 $K_i=677$ nM)²⁶ were obtained from Cayman Chemical (Ann Arbor, MI).

Drugs were dissolved in 10% DMSO, 10% Tween-80, and 80% saline (vehicle Sigma) with an injection volume of 10 mL/kg; doses are given in Table 1.

Western blot

Tissue samples were prepared with lysis buffer (20 mM Tris-HCl [pH 7.4], 50 mM NaCl, 2 mM MgCl₂ hexahydrate, 1% [v/v] NP40, 0.5% [w/v] sodium deoxycholate, 0.1% [w/v] sodium dodecyl sulfate [SDS]) and supplemented with protease inhibitor (Bimake B14002) and phosphatase inhibitor (Bimake B15002).

Tissues were sonicated (Sonic Dismembrator Model100; Fisher) at a strength of five for five pulses, three times each. Samples were centrifuged at 13,000 g for 10 min at 4°C to separate solid particles, and Tris-Glycine

Table 1. Table of Drugs Used, Receptor Targets, Affinity (-ies), Dose, and Brain Penetration

Drug	Receptor	Affinity (K _i)	Dose
Morphine	Mu	K _i = 1.1 nM (Khroyan et al. ¹⁹)	1 mg/kg 10 mg/kg 30 mg/kg 100 mg/kg
AM2301	CB2	CB2 K _i = 1.3 nM, CB1 K _i = 172 nM (Unpublished data)	1 mg/kg 10 mg/kg 30 mg/kg 100 mg/kg
SR-144528	CB2	CB2 K _i = 0.6 nM CB1 K _i = 400 nM (Rinaldi-Carmona et al. ²²)	10 mg/kg
AM630	CB2	CB2 K _i = 32.1 nM CB1 K _i = 5152 nM (Cayman chemical)	10 mg/kg
AM356	CB1	CB1 K _i = 37 nM, CB2 K _i > 1,000 nM (Liu et al. ²⁰)	1 mg/kg 10 mg/kg
THC	CB1/CB2	CB1 K _i = 48 nM, CB2 K _i = 40 nM (Nikas et al. ²⁴)	1 mg/kg 10 mg/kg
JWH 133	CB2	CB2 K _i = 3.4 nM CB1 K _i = 677 nM (Cayman chemical)	10 mg/kg

THC, Δ⁹-tetrahydrocannabinol.

eXtended (10% Criterion™; BioRad) precast gels were loaded with 10 μg of total protein from the supernatant, separated by SDS-PolyAcrylamide Gel Electrophoresis, and transferred to Amersham Protran nitrocellulose blotting membranes (No. 10600001; GE Health Care, St. Louis, MO) then blocked for 1 h in 5% bovine serum albumin (BSA) in tris-buffered saline with Tween 20 (TBST) at room temperature. Antibodies were diluted in 5% BSA in TBST (Table 2). Primary antibody was washed thrice in TBST before secondary antibody incubation (Lincoln, NE).

Membranes were imaged using LiCor Odyssey infrared imaging system (LiCor, Lincoln, NE). Images were quantified using Un-Scan-It gel version 6.1 scanning program (Silk Scientific). Protein expression was normalized to expression of β-actin.

Quantitative real-time PCR

All procedures were performed simultaneously by one experimenter to prevent interexperiment variability. Total RNA was extracted from the tissue using RNeasy Mini Kit (No. 74104) from Qiagen (Germantown, MD) per the manufacturer's protocol, with final reconstitution of the RNA in nuclease-free water and storage at -80°C until analysis. The RNA was quantified using a NanoDrop ND-1000 Spectrophotometer (ThermoFisher). Single-stranded complementary DNA (cDNA) was synthesized using high-capacity cDNA reverse transcription kit (27-874-06) from Fisher Scientific, following the manufacturer's protocol.

The amplified cDNA was added to the RT² SYBR Green Master Mix (No. 330500; Qiagen) and gene specific primers. RT² qPCR primer assays (No. 330001; Qiagen) detected the expression of *CNRI*, CB1 gene, (PPM04603A), *CNR2*, CB2 gene, (PPM04826A), and *OPRM1*, MOR gene, (PPM04257G) genes. The sequence for these was a 5' 3' primers designed to flank intronic sequences to identify genomic DNA contamination and was analyzed by Basic Local Alignment Search Tool (BLAST) to confirm target selectivity.

The following primers were used to quantify the expression of glyceraldehyde phosphate dehydrogenase (GAPDH): Forward—5' TCC TGC ACC ACC AAC TGC TTA G 3' (No. 191151516); GAPDH-Reverse—5' GAT GAC CTT GCC CAC AGC CTT G 3' (No. 191151517) Integrated DNA Technologies (Coralville, Iowa). GAPDH primers flank intronic sequences to identify genomic DNA contamination and analyzed by BLAST to confirm target selectivity.

The quantitative PCR (qPCR) was performed on the Lightcycler 96 Real-Time PCR System (Roche, Indianapolis, IN), using the thermal program: 95°C for 10 min, 45 cycles of 95°C for 15 sec, and 60°C for 1 min and a melt curve analysis. The melt curves were analyzed to confirm selectivity and supported by

Table 2. Table of Antibodies Used, Supplier, Dilutions, and Assay Used With

Antibody	Supplier	Dilution	Western blot
Rabbit-anti-MOR antibody—N—terminal	Abcam no. ab137460	1:500 1:5000	Yes
Rabbit-anti-CB2 antibody—N—terminal	Abcam no. ab3561	1:500 1:1000	Yes
Rabbit-anti-CB1 antibody	Abcam no. ab186428	1:500 1:1000	Yes
β-actin	Cell Signaling mAB no. 3700 (8H10D10)	1:10,000	Yes
Goat antimouse IgG (H+L)	LI-COR IRDye680LT (NC0046410)	1:10,000	Yes
Goat antirabbit IgG (H+L)	LI-COR IRD800CW (NC9401842)	1:10,000	Yes

MOR, mu opioid receptor; CB2, cannabinoid-2 receptor; CB1, cannabinoid-1 receptor; IgG, immunoglobulin G.

agarose gel electrophoresis. Cycle thresholds (Ct) normalized to GAPDH Ct generated relative gene expression of each target.

Statistical analysis

Numbers required to generate 80% statistical power were determined with GPower 3.1 for all experiments.²⁸ GraphPad Prism 8.0 software performed analysis for statistical significance. All data were expressed as mean \pm standard error of the mean (SEM). Multiple comparisons two-way analyses of variance (ANOVAs) analyzed differences between groups for respiratory depression, allodynia, and tail flick with Bonferroni tests applied *post hoc*. Allodynia and tail flick data are expressed as area under the curve (AUC) \pm SEM for withdrawal latency with differences assessed by an unpaired *t*-test with the Welch's correction. Western blots and qPCR were compared utilizing one-way ANOVA. A *p*-value of <0.05 was considered statistically significant.

Results

MS-induced respiratory depression

MS produces respiratory depression^{29,30} at antinociceptive doses.⁷ To validate MS depression, 1, 3, 10, or 30 mg/kg (i.p., $N \geq 6$ /group) was compared with vehicle (i.p., $N=11$; Fig. 1A; $F[4,819]=65.61$, $p < 0.0001$). Doses of 10, 30, 100 and 300 mg/kg showed significant suppression of BPM under both CO₂ conditions ($F[20,819]=11.34$, $p < 0.0001$); tidal volume was not affected (Supplementary Fig. S2). The AUC for each MS dose was calculated in each condition. Comparison of MS AUCs 10, $p=0.0033$, 30, $p=0.0004$, 100, $p=0.0008$, and 300 mg/kg, $p=0.0082$, under the 0% CO₂ and MS 10, $p < 0.0001$, 30, $p=0.0002$, 100, $p < 0.0001$, and 300 mg/kg, $p < 0.0001$, under the 5% CO₂ condition (100 and 300 mg/kg data not shown) induced significant respiratory depression compared with vehicle (Fig. 1B).

Cannabinoids and respiration

THC (1, 10 mg/kg, i.p., $N=9$ /group), a mixed CB1R/CB2R agonist, doses were chosen based on published reports.³¹⁻³³ THC was compared with vehicle and was significant for a factor of dose ($F[2,52]=4.245$, $p=0.0196$). THC 1, $p > 0.9999$ under both conditions, and 10 mg/kg, $p=0.4098$, did not significantly decrease frequency of respirations, or BPM, under the 0% CO₂ condition (Fig. 2A) compared with vehicle (from Fig. 1B), but under 5% CO₂, THC 10 mg/kg, $p=0.0272$, did show a reduction in BPM (Fig. 2B).

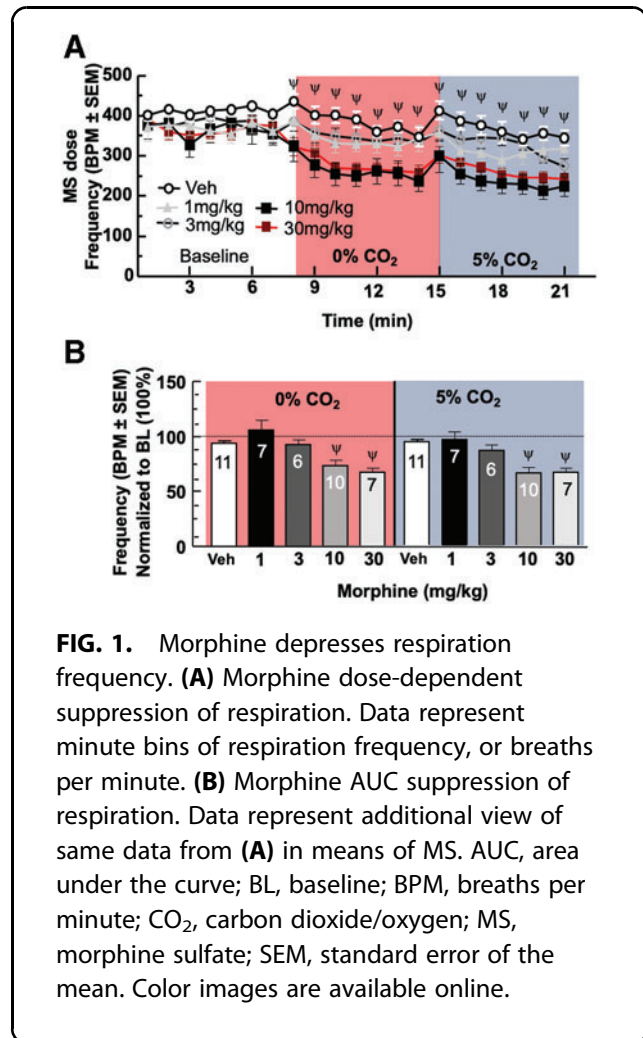
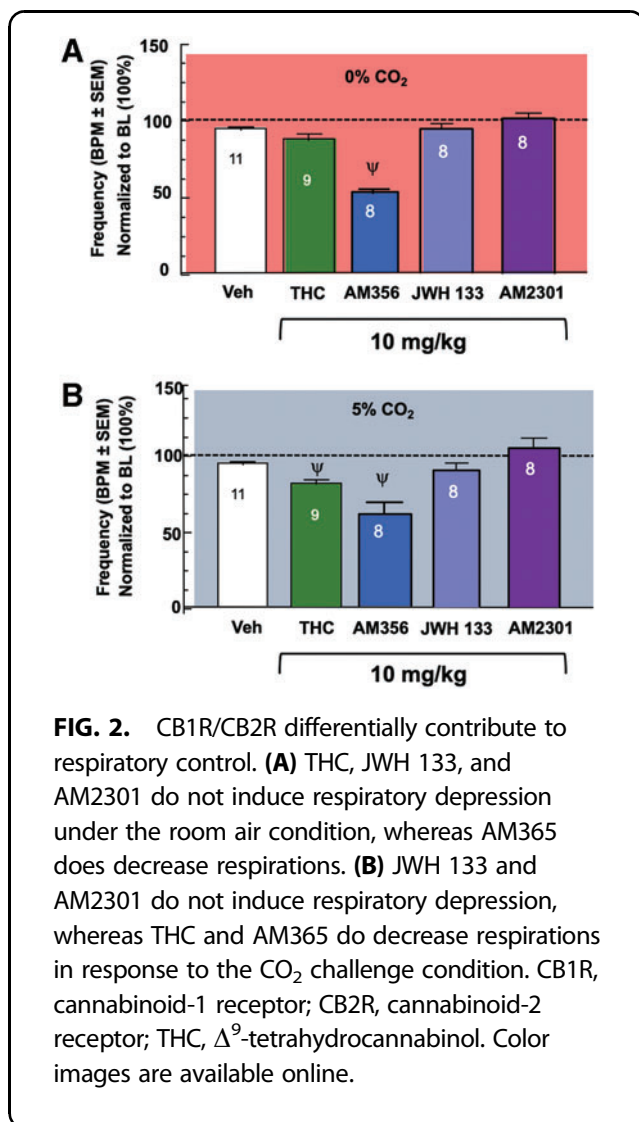


FIG. 1. Morphine depresses respiration frequency. **(A)** Morphine dose-dependent suppression of respiration. Data represent minute bins of respiration frequency, or breaths per minute. **(B)** Morphine AUC suppression of respiration. Data represent additional view of same data from **(A)** in means of MS. AUC, area under the curve; BL, baseline; BPM, breaths per minute; CO₂, carbon dioxide/oxygen; MS, morphine sulfate; SEM, standard error of the mean. Color images are available online.

The synthetic CB1R agonist, AM356, as a factor of drug ($F[2,46]=52.03$, $p < 0.0001$) at 1 mg/kg, $p=0.0589$ room air and $p > 0.9999$ CO₂, ($N=8$) did not significantly decrease BPM, although 10 mg/kg, $p < 0.0001$, ($N=8$) did significantly decrease BPM, doses determined based on prior literature,²⁰ and by a factor of CO₂ condition ($F[1,46]=5.933$, $p=0.0188$; Fig. 2A, B). In contrast, the highly synthetic CB2R agonist, JWH 133, (10 mg/kg, $N=8$) did not significantly decrease respiratory rates regardless of CO₂ condition, $p > 0.9999$ (Fig. 2A, B). Similarly, a novel selective CB2R agonist, AM2301,³⁴ ($F[3,62]=0.4802$, $p=0.6972$; 1, $p > 0.9999$, 10 mg/kg, $p=0.4397$, $N=8$) did not significantly decrease BPM under either CO₂ condition (Fig. 2A, B).

AM2301 on MS-induced respiratory depression

A multiple comparisons two-way ANOVA was conducted to compare the effects of AM2301 in a dose-



dependent manner in combination with MS ($F[8,118] = 23.27$, $p < 0.0001$) and CO₂ condition ($F[1,118] = 9.441$, $p = 0.0026$). AM2301 (10 mg/kg i.p.) significantly attenuated 10 mg/kg MS-induced respiratory depression under room air, $p = 0.0257$, and the CO₂ condition, $p < 0.0001$ (Fig. 3A).

The 1:3 (AM2301:MS) combination was not significantly different than MS, $p > 0.9999$, in the room air condition and in the 5% CO₂ condition. In addition, the 1:10 combination of AM2301 and MS had no impact on the MS-induced respiratory depression under either condition when compared with MS, $p > 0.9999$ for room air and 5% CO₂. The 1:1 (AM2301:MS) combination of 30 mg/kg showed statistically similar respiratory depression under room air, $p > 0.9999$, compared with MS in both conditions. Finally, the

100 mg/kg combination of AM2301 and MS had no impact on the MS-induced respiratory depression, $p > 0.9999$ compared with MS, either condition (Fig. 3A).

Analysis of dose dependency revealed that AM2301 maintained BPM at all doses, whereas MS showed dose-dependent reductions in respirations compared with vehicle (Fig. 3B). Combinations of AM2301 10 mg/kg alongside escalating MS doses showed a rightward shift of the dose response curve (Figs. 3B, C).

Actions of CB inverse agonists on respiratory depression

A multiple comparisons two-way ANOVA was utilized to evaluate multiple inverse agonists for a factor of drug ($F[4,74] = 13.86$, $p < 0.0001$). Respiratory depression was induced by AM630 10 mg/kg,^{35,36} ($N = 7$) under the 5% CO₂, $p = 0.0328$, but not under room air, $p = 0.2444$. The inverse agonist, SR-144528, at 10 mg/kg induced respiratory depression on its own ($N = 8$) in room air $p = 0.0012$ and 5% CO₂ $p = 0.0315$. Additionally, when SR-144528 was administered following JWH 133 (10 mg/kg; Fig 4B) or MS (10 mg/kg; Fig. 4C), respiratory depression was also seen regardless of air condition. Interestingly, administration of SR-144528 did not exacerbate respiratory depression induced by AM356, which was able to be reversed with the CB1 inverse agonist, SR-141716A (Fig. 4D).

A multiple comparisons two-way ANOVA was utilized to evaluate multiple inverse agonists after morphine administration and an interaction was seen between time and drug ($F[3,50] = 5.187$, $p = 0.0034$). Administration of the CB2 inverse agonist, SR-144528 10 mg/kg or AM630 10 mg/kg, after administration of MS (from Fig. 1B) had no impact on the MS-induced respiratory depression, $p > 0.9999$, in both conditions.

A multiple comparisons two-way ANOVA was utilized to evaluate multiple inverse agonists after CB1 activation and an interaction was seen between time and drug ($F[3,50] = 3.127$, $p = 0.0339$). Administration of the CB1 inverse agonist, SR-141718A 10 mg/kg, after administration of AM356 10 mg/kg, significantly reversed the respiratory depression induced by AM356 in both CO₂ conditions, $p < 0.0001$, compared with AM356. Administration of the CB2 inverse agonist, SR-144528 10 mg/kg, after administration of AM356 increased the mean BPM in both CO₂ conditions, but was only significantly higher than AM356 alone in room air, $p = 0.0246$, and statistically comparable with AM356 in the 5% CO₂ condition, $p > 0.9999$.

A multiple comparisons two-way ANOVA was utilized to evaluate the inverse agonists, SR-141718A

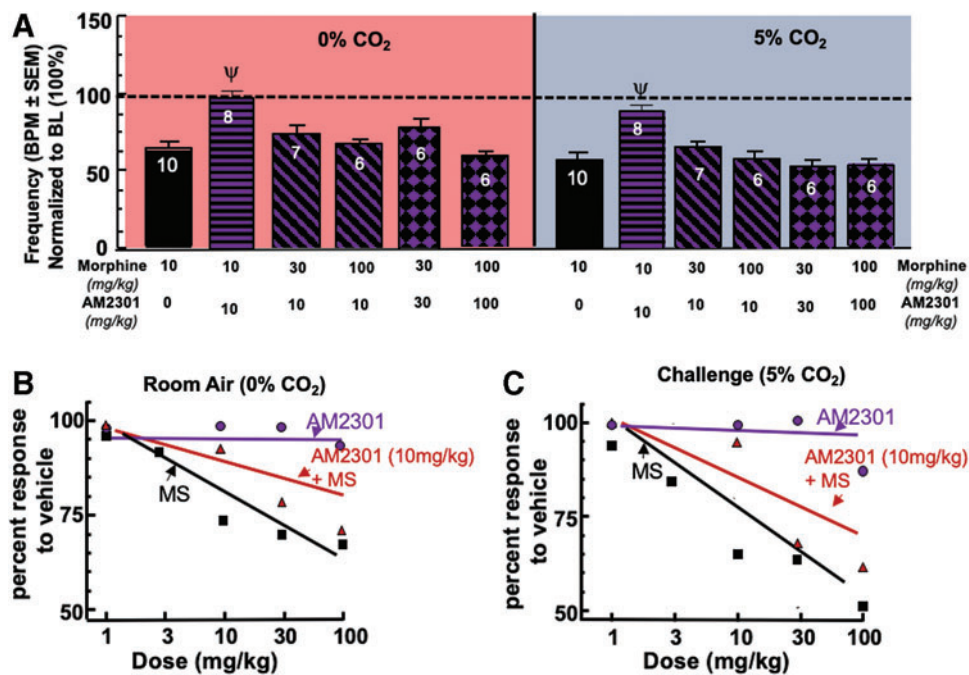


FIG. 3. AM2301 influence on respirations with MS. **(A)** Attenuation of morphine-induced respiratory depression through CB2 activation. The combination of AM2301 (10 mg/kg) and MS (10 mg/kg) significantly prevented respiratory depression compared with MS, whereas AM2301 (10 mg/kg) failed to decrease 30 or 100 mg/kg MS-induced respiratory depression in either CO₂ condition. Increasing the AM2301 dose (30 mg/kg) failed to decrease 30 mg/kg MS-induced respiratory depression and an increase to 100 mg/kg failed to overcome 100 mg/kg MS-induced respiratory depression in either CO₂ condition as well. **(B)** Room air respiratory dose–response curves. Dose–response curves for AM2301, MS, and AM2301 10 mg/kg plus escalating doses of MS were developed using this nonlinear regression equation $Y = 100 / (1 + 10^{\{[\text{LogEC}_{50} - X] \times \text{HillSlope}\}})$. **(C)** 5% CO₂ respiratory dose–response curves. Dose–response curves for AM2301, MS, and AM2301 10 mg/kg plus escalating doses of MS were developed using this nonlinear regression equation $Y = 100 / (1 + 10^{\{[\text{LogEC}_{50} - X] \times \text{HillSlope}\}})$. Color images are available online.

10 mg/kg, AM630 10 mg/kg, and SR-144528 10 mg/kg, for a factor of drug ($F[7,116] = 21.17$, $p < 0.0001$). AM630 significantly reversed the mitigation of opioid-induced respiratory depression when administered after the AM2301 + MS combination (from Fig. 3A) under both CO₂ conditions compared with MS 10 mg/kg alone (from Fig. 1B), room air, $p = 0.1708$, 5% CO₂, $p > 0.9999$ (Fig. 4E). In addition, a depression comparable with the administration of MS 10 mg/kg alone was seen under both CO₂ conditions following the administration of SR-144528 (Fig. 4E).

MOR, CB1R, and CB2R expression in the preBötzinger Results thus far suggest CB2 receptors are necessary for maintaining respiratory homeostasis, so we wanted to investigate the respiratory nuclei, the pBc,

for their presence. Expression of CBRs in pBc is today poorly documented. Quantitative real-time PCR (RT-PCR) detected *CNR1*, *CNR2*, and *OPRM* messenger RNA in the pBc ($N = 3$; Fig. 5A); spleen and PAG served as positive controls (Fig. 5B, C). Total protein expression of pBc MOR, CB1R, and CB2R ($N = 3$ pools of four mice) was measured using Western blotting; each receptor was detected. The positive control, PAG,³⁷ for MOR and CB1 showed statistically equivalent concentrations to the pBc (Fig. 5D, E). The positive control for CB2, spleen,³⁸ revealed a statistically equivalent expression in the pBc (Fig. 5D, E).

Retention of antinociception in the tail-flick assay Administration of AM2301 10 mg/kg, MS 10 mg/kg, vehicle, and the combination of AM2301 10 mg/kg + MS 10 mg/kg following a baseline reading (Fig. 6A,

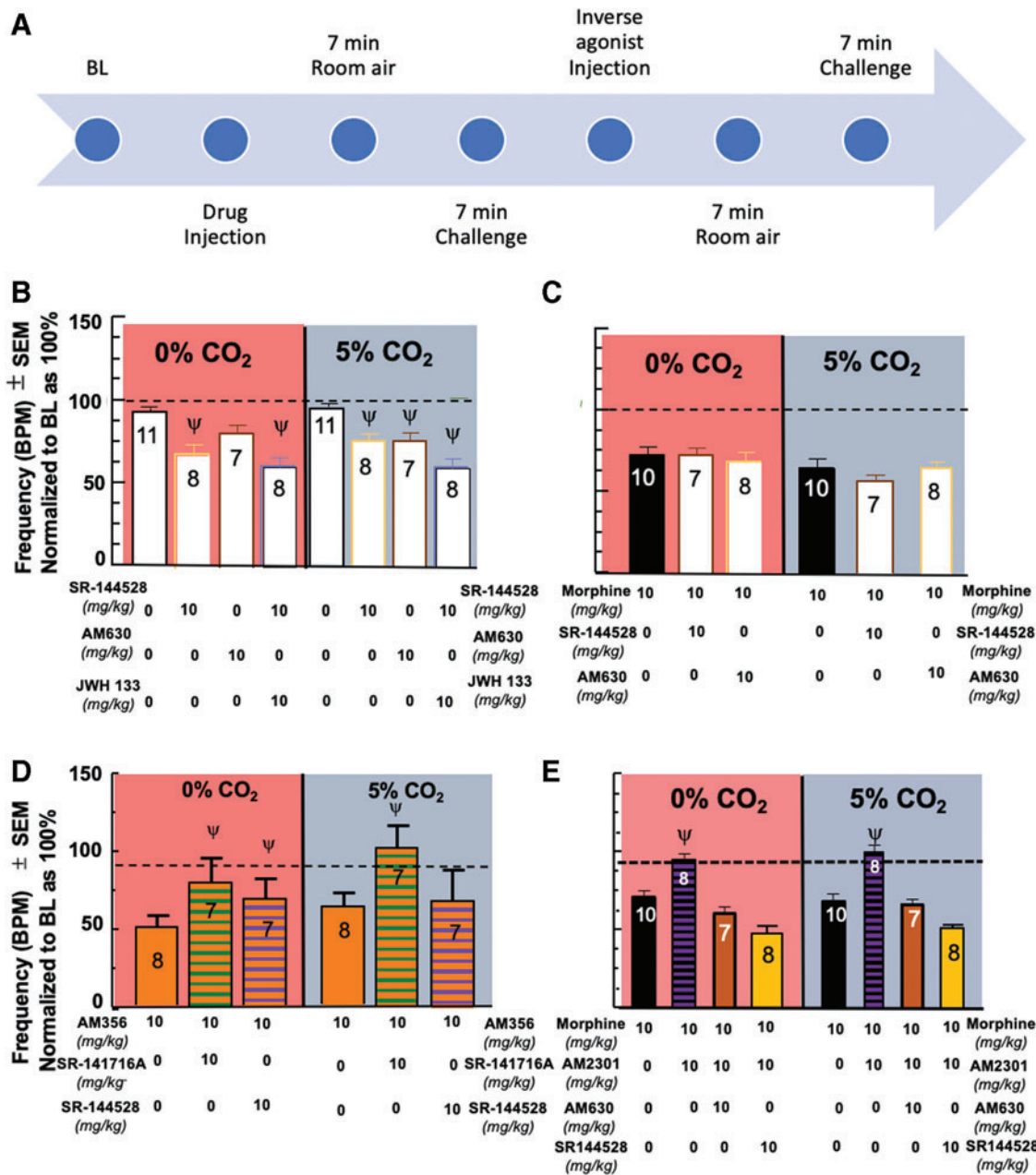


FIG. 4. Effects of CB inverse agonists on respirations and reversal of morphine-induced respiratory depression mitigation. **(A)** Inverse agonist timeline. After completion of the initial timeline, an injection of the inverse agonist is administered and followed by a repeat of the CO₂ conditions to evaluate reversal of the previously administered compound. **(B)** CB2 inverse agonism induces respiratory depression. SR-144528 10 mg/kg, a CB2 inverse agonist, induced respiratory depression on its own. AM630 10 mg/kg, a CB2 inverse agonist, induced respiratory depression under the 5% CO₂ condition, but not under room air. Administration of SR-144528 10 mg/kg after JWH 133 10 mg/kg was able to induce respiratory depression in both air conditions. **(C)** MS respiratory depression not impacted by administration of CB2 inverse agonism. Administration of the CB2 inverse agonist, SR-144528 10 mg/kg or AM630 10 mg/kg, after administration of MS (from Fig. 1B) had no impact on the MS-induced respiratory depression. **(D)** AM356-induced respiratory depression reversed by administration of CB1 inverse agonism. Administration of the CB1 inverse agonist, SR-141718A 10 mg/kg, after administration of AM356 10 mg/kg significantly reversed the respiratory depression induced by AM356 in both CO₂ conditions. Administration of the CB2 inverse agonist, SR-144528 10 mg/kg, after administration of AM356 increased the mean BPM in both CO₂ conditions, but was only significantly higher than AM356 alone in room air. **(E)** Reversal of AM2301 mitigation of opioid-induced respiratory depression with CB2 inverse agonists. AM630 (10 mg/kg; *N*=7/group) and SR-144528 (10 mg/kg; *N*=8/group) significantly reversed the AM2301 mitigation of MS-induced respiratory depression. Color images are available online.

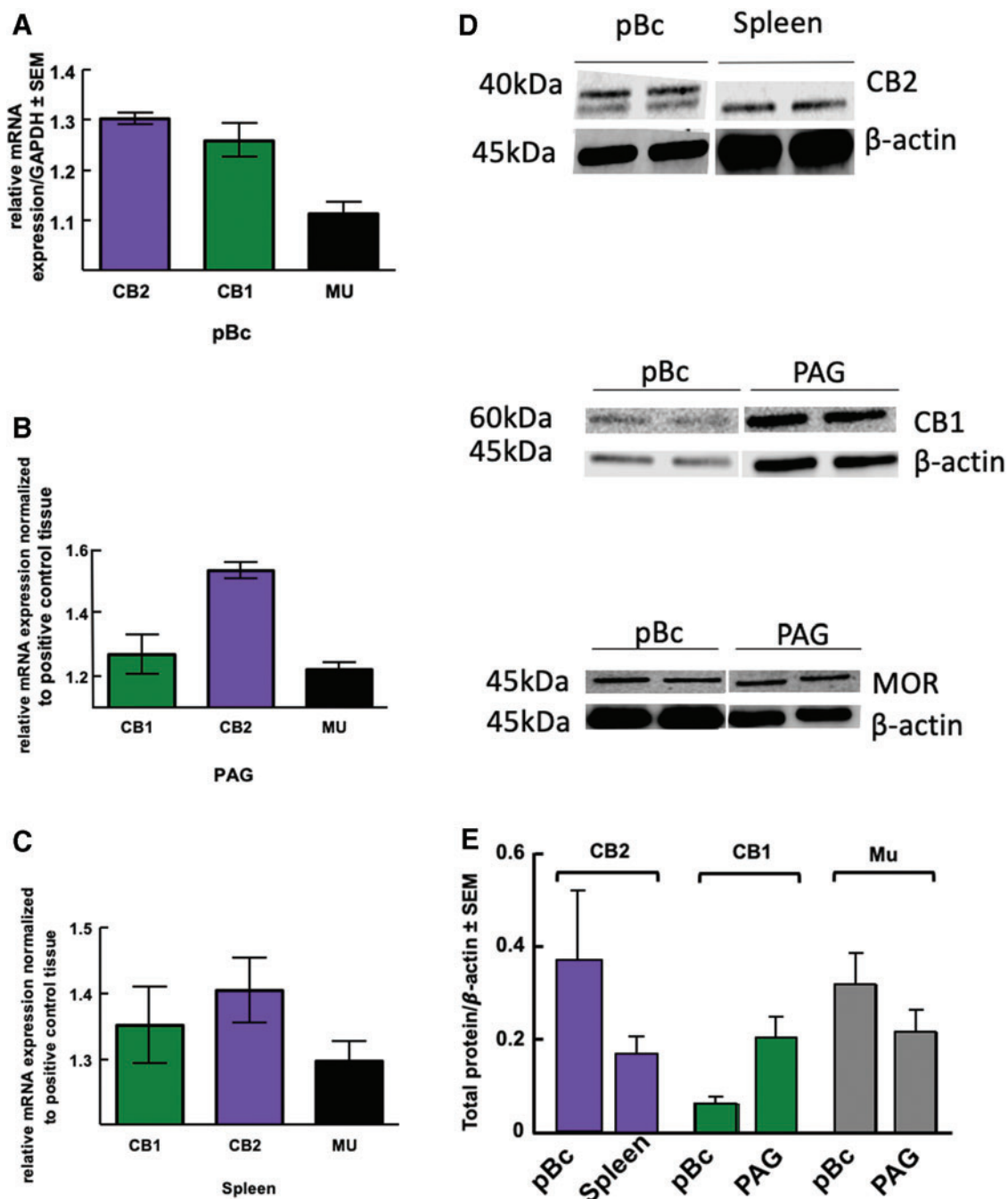


FIG. 5. Total expression of Mu, CB1R, and CB2R in the preBötzing. **(A)** Using qPCR to measure mRNA levels, *CNR2* and *CNR1* were present in the pBc, as well as *OPRM* **(B)** Relative mRNA expression showed the presence of *CNR1*, *CNR2*, and *OPRM* in the PAG. **(C)** mRNA levels within the spleen were assessed using qPCR, and *CNR1*, *CNR2*, and *OPRM* were all found. **(D)** Membrane images of the Western blots are analyzed in the next panel. **(E)** Western blots were used to measure protein levels of MOR, CB1, and CB2 in pBc samples ($n = 3$). Protein expression of MOR and CB1 was compared with PAG-positive control tissue, whereas CB2 was compared with spleen. Protein levels showed a spleen-equivalent concentration of CB2R expression, as well as MOR and CB1R expression. MOR, mu opioid receptor; mRNA, messenger RNA; PAG, periaqueductal gray; pBc, preBötzing complex; qPCR, quantitative PCR. Color images are available online.

B) before administration of any compound ($N=9-11$ per group) was conducted and an interaction was seen between the effects of drug and time ($F[18,175]=2.989$, $p<0.0001$).

The combination of AM2301 + MS, $p=0.0028$, and MS, $p=0.0254$, alone showed greater antinociceptive effects when compared with vehicle and AM2301, $p=0.9690$, alone at 15 min after drug administration. The combination of AM2301 and MS, 30 min $p=0.0002$, 45 min $p=0.0003$, 60 min $p<0.0001$, and MS, 30 min $p<0.0001$, 45 min $p<0.0001$, 60 min $p=0.0189$, alone showed an equal increase in antinociceptive effects when compared with vehicle until the 90-min time point, at which time the combination of AM2301 and MS, $p<0.0001$, was statistically significantly more antinociceptive compared with MS alone, $p=0.2036$, showing a longer time of antinociceptive effects than MS when compared with vehicle and AM2301, $p=0.7657$, on its own.

All groups returned to baseline tail-flick latencies at the 120-min, $p>0.9999$, mark postdrug administration. Calculated AUC (Fig. 6B) confirmed effects of MS and AM2301 + MS as compared with controls.

Evaluation of postoperative pain after AM2301 + MS administration

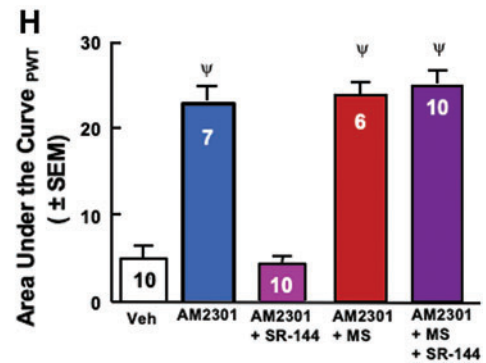
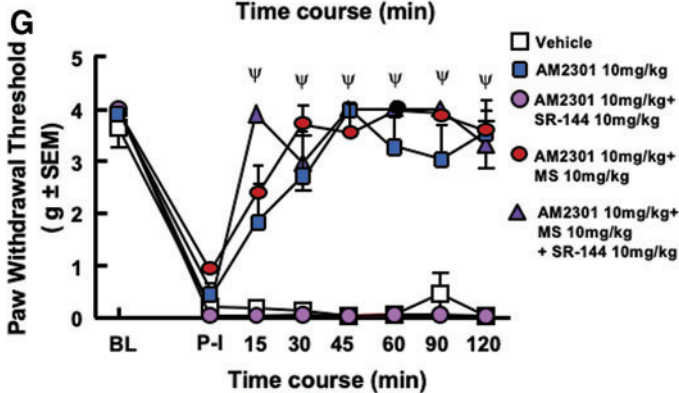
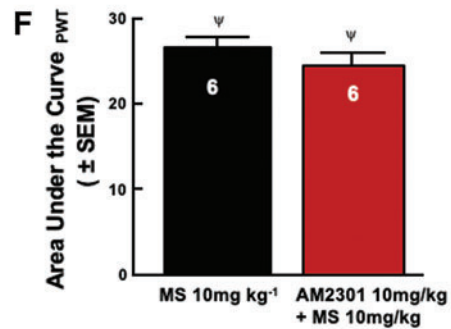
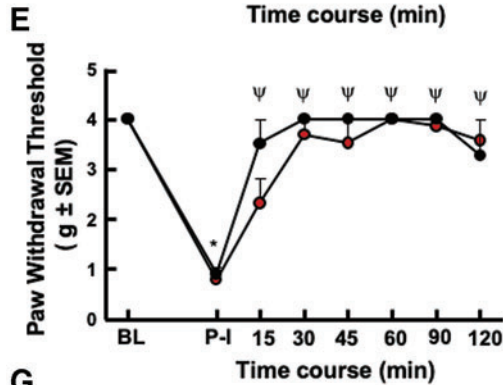
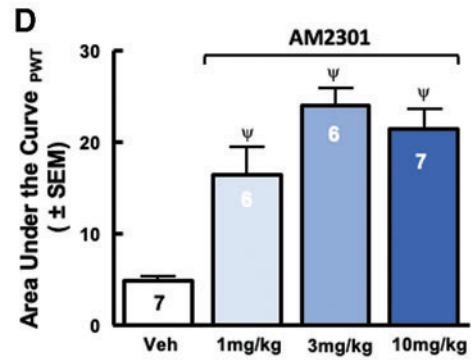
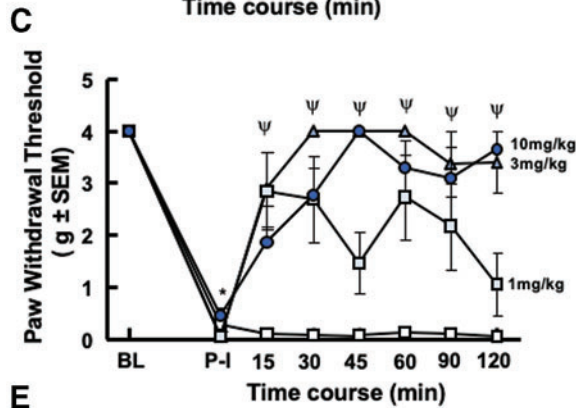
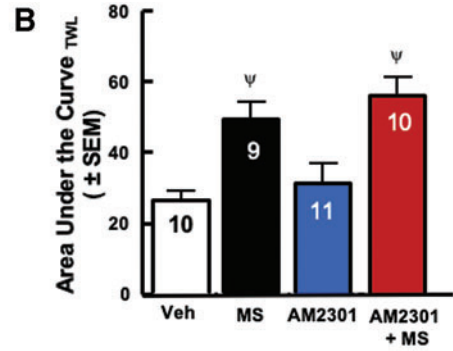
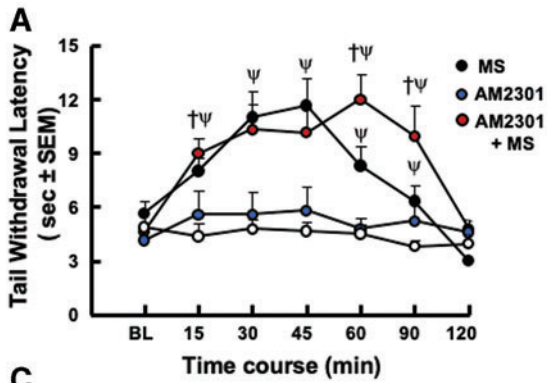
Mice showed significant decreases in paw withdrawal thresholds of injured paw 24 h postincision (Fig. 6C, E, G). A multiple comparisons two-way ANOVA was

conducted, and an interaction was seen between the effects of drug and time ($F[21,168]=4.650$, $p<0.0001$). AM2301 ($N=6-7$ per group; 3, $p<0.0001$, and 10 mg/kg, $p<0.0001$.) was significantly more efficacious when compared with vehicle at all time points after drug administration (Fig. 6C). AM2301 1 mg/kg was efficacious at all time points, $p<0.0001$, 90 min $p=0.0023$, except 45, $p=0.0691$, and 120 min, $p=0.02923$.

A multiple comparisons two-way ANOVA was conducted, and an interaction was seen between the effects of drug and time ($F[14,128]=14.23$, $p<0.0001$). The combination of AM2301 10 mg/kg, $p<0.0001$, and MS 10 mg/kg, $p<0.0001$, was equal to MS alone in antinociceptive effects (Fig. 6E, F) at all time points compared with vehicle from panel D after drug administration.

A combination of MS (10 mg/kg) and AM2301 (10 mg/kg; $N=6$) retained antihypersensitive effects for the testing duration (Fig. 6E); administration of SR-144528 10 mg/kg 10 min before the administration of vehicle, AM2301 10 mg/kg, or AM2301 10 mg/kg + MS 10 mg/kg was conducted (Fig. 6G) and an interaction was seen between the effects of drug and time ($F[35,352]=14.70$, $p<0.0001$) that prevented the reversal of hypersensitivity by AM2301 alone, $p>0.9999$ at all time points, but had no impact on vehicle, $p>0.9999$ at all time points, or AM2301 + MS combination, $p<0.0001$ at all time points, administration throughout the time course (Fig. 6G, H).

FIG. 6. AM2301, a brain penetrant CB2R agonist retains antinociceptive and antiallodynic properties in combination with morphine. **(A)** Tail-flick antinociception. AM2301 + MS showed equiefficacious antinociception versus MS alone. All groups returned to baseline tail-flick latencies 120 min postdrug administration with peak drug effect between 45 and 60 min. **(B)** Tail flick area under the curve. AM2301 in combination with MS showed equal increases in statistical significance in the AUC as MS compared with vehicle or AM2301 alone. **(C)** Postoperative pain evaluation of AM2301 dose-response after paw incision through von Frey assay. After postinjury baseline, AM2301 ($N=6-7$ /group) demonstrated a significant increase in thresholds. **(D)** Postoperative pain evaluation of AM2301 area under the curve. Compared with vehicle, AM2301 at all doses showed statistically significant increases in AUC. **(E)** Postoperative pain evaluation of AM2301 + morphine and morphine alone after paw incision through von Frey assay. MS administration ($N=6$) significantly reversed postoperative mechanical hypersensitivity. A combination of MS (10 mg/kg) and AM2301 (10 mg/kg; $N=6$) retained antihypersensitive effects for the testing duration. **(F)** Postoperative pain evaluation of AM2301 + morphine and morphine alone area under the curve. Compared with vehicle from **(D)**, the combination AM2301 with MS and MS alone showed statistically significant increases in AUC. **(G)** Reversal of AM2301 antinociception with a CB2 inverse agonist. Pretreatment with a CB2R inverse agonist, SR-144528, (10 mg/kg), 10 min before AM2301 alone or in combination with MS, ($N=10$ /group) significantly mitigated the antihyperalgesia of AM2301, yet, the AM2301 + MS antihyperalgesia was not significantly prevented. **(H)** CB2 inverse agonist reversal of AM2301 antinociception area under the curve. Administration of SR-144528 10 mg/kg before drug administration showed a prevention for AM2301-induced antinociception back to postincision baseline while having no impact on the antinociception induced by the combination of AM2301 and MS. Color images are available online.



Discussion

Most fatal opioid overdoses result from respiratory depression, necessitating alternative or adjunct interventions to limit this adverse event.³⁹ These studies demonstrate CB2R agonism, AM2301, with MS, does not alter analgesia or antihyperalgesia efficacy of MS but, importantly and significantly, prevents respiratory depression in the 1:1 10 mg/kg dose. Although AM2301 had no antinociceptive efficacy as expected,⁷⁻⁹ AM2301 antihyperalgesia was dose dependent and time dependent against postsurgical pain, similar to previous studies demonstrating that CB2R agonists are more effective in inflammatory and chronic pain.⁷⁻⁹ The CB2R antagonist, SR-144528, blocked the antihyperalgesic effects of AM2301, supporting a CB2R mechanism of action.

To delineate the role of different cannabinoids on respiration, nonselective and selective CB1R and CB2R agonists including THC, AM356, JWH 133, and AM2301 were studied. The synthetic cannabinoid AM356, a selective CB1R agonist, induced respiratory depression and these effects were reversed after administration with the CB1 inverse agonist, SR-141716A. Synthetic cannabinoids have shown respiratory depression,⁴⁰ including here with THC, a mixed CB1R/CB2R agonist. Finally, the CB2R selective agonists, JWH 133 and AM2301, did not significantly induce respiratory depression. Yet, studies here for the first time demonstrated that the novel CB2R agonist, AM2301, significantly prevented MS-induced respiratory depression at the 1:1 combination of 10 mg/kg in both room air and 5% CO₂ conditions.

CB1R presence in the pBc suggests that isolated CB1 activation in the pBc may cause respiratory depression seen with AM356. Given that CB1R couples to G α_i , like MOR, hyperpolarizing the neurons through G-protein inward rectifying potassium channel activation may explain reduction of CB1R agonists in respiration. Notably, studies here demonstrated selective CB2R agonism with AM2301 significantly prevented MS-induced respiratory depression at the 1:1 10 mg/kg combination. The high dose MS-induced respiratory depression was insensitive to AM2301, likely reflecting increased occupancy of MORs, suggesting CB2 saturation and nonspecific binding driving the reduction in BPM.

Quantitative RT-PCR confirmed that the pBc, a central nervous system (CNS) nucleus critical for spontaneous inspiratory rhythm, is populated with CB2R, more so than MOR and almost four times more than CB1R and equivalently to levels of CB2R measured in the spleen, but it is worth mentioning that the full spleen was evaluated in comparison with the single pBc nucleus

that would have otherwise shown a reduced concentration if the whole brain had it been compared with the spleen.

Studies in mice and rats in the reward centers of the CNS using CB2R selective agonists have demonstrated inhibiting and reversing the effects of CB1 and MOR activity.⁷ Although limited knowledge of endocannabinoids (ECs) within the pBc exists, studies here revealed significant respiratory depression using a CB2R inverse agonist suggesting tonic EC activity of CB2Rs in normal respiratory physiology. Thus, the lack of increase in BPM from AM2301 alone is unsurprising, as ECs are already modulating the basal respiratory rate. Finally, the differences observed between selective synthetic cannabinoids versus the phytocannabinoid THC's multitargeted mechanisms of action may be explained by promiscuity of CBR binding.

In conclusion, these studies support a role for cannabinoids to influence respiratory drive physiologically and during opioid exposure. Respiratory frequency was depressed partially by THC and AM356, but not JWH 133 or AM2301. Selective CB2R activation with AM2301 significantly mitigated MS-induced respiratory depression in male mice. As these were the initial studies, future studies will need to investigate potential gender differences, repeating each experiment in females. Thus, distinct targeting of CB2R with structurally defined compounds has potential to reduce opioid risks while increasing or maintaining analgesic efficacy.

Author Disclosure Statement

The authors declare no competing financial interests.

Funding Information

This study was supported by National Institutes of Health/National Institute of Drug Abuse funding to T.W.V. (1P01DA041307-01), A.M. (DA 009158, DA 045020, DA 05801, and DA 041307), National Cancer Institute (R01CA142115-02), Comprehensive Pain and Addiction Center (CPAC), and University of Arizona Health Sciences. The Zeiss Elyra S.1 microscope, Imaging Cores—Life Sciences North, University of Arizona's Arizona Research Labs (purchase supported by NIH S10 OD019948).

Supplementary Material

Supplementary Figure S1

Supplementary Figure S2

References

1. NASEM. Pain management and the opioid epidemic: balancing societal and individual benefits and risks of prescription opioid use. The National Academies Press: Washington, DC, 2017.

2. Markos JR, Harris HM, Gul W, ElSohly MA, Sufka KJ. Effects of cannabidiol on morphine conditioned place preference in mice. *Planta Medica*. 2018; 84:221–224.
3. Control CfD, Prevention. Understanding the epidemic. 2017;11. Available at <https://www.cdc.gov/drugoverdose/epidemic/index.html> Accessed October 15, 2020.
4. Dahan A, Aarts L, Smith TW. Incidence, reversal, and prevention of opioid-induced respiratory depression. *Anesthesiology*. 2010;112:226–238.
5. Bradford AC, Bradford WD, Abraham A, et al. Association between US state medical cannabis laws and opioid prescribing in the Medicare Part D population. *JAMA Intern Med*. 2018;178:667–672.
6. Webster L, Schmidt WK. Dilemma of addiction and respiratory depression in the treatment of pain: a prototypical endomorphin as a new approach. *Pain Med*. 2019;21:992–1004.
7. Grenald SA, Young MA, Wang Y, et al. Synergistic attenuation of chronic pain using mu opioid and cannabinoid receptor 2 agonists. *Neuropharmacology*. 2017;116:59–70.
8. Ibrahim MM, Porreca F, Lai J, et al. CB2 cannabinoid receptor activation produces antinociception by stimulating peripheral release of endogenous opioids. *Proc Natl Acad Sci USA*. 2005;102:3093–3098.
9. Lin X, Dhopeswarkar AS, Huibregtse M, et al. Slowly signaling G protein-biased CB2 cannabinoid receptor agonist LY2828360 suppresses neuropathic pain with sustained efficacy and attenuates morphine tolerance and dependence. *Mol Pharmacol*. 2018;93:49–62.
10. Lozano-Ondoua AN, Hanlon KE, Symons-Liguori AM, et al. Disease modification of breast cancer-induced bone remodeling by cannabinoid 2 receptor agonists. *J Bone Mineral Res*. 2013;28:92–107.
11. Yuill MB, Hale DE, Guindon J, et al. Anti-nociceptive interactions between opioids and a cannabinoid receptor 2 agonist in inflammatory pain. *Mol Pain*. 2017;13:1744806917728227.
12. Reiman A, Welty M, Solomon P. Cannabis as a substitute for opioid-based pain medication: patient self-report. *Cannabis Cannabinoid Res*. 2017;2:160–166.
13. Boehnke KF, Litinas E, Clauw DJ. Medical cannabis use is associated with decreased opiate medication use in a retrospective cross-sectional survey of patients with chronic pain. *J Pain*. 2016;17:739–744.
14. Gruber SA, Sagar KA, Dahlgren MK, et al. Splendor in the grass? A pilot study assessing the impact of medical marijuana on executive function. *Front Pharmacol*. 2016;7:355.
15. Lowery JJ, Raymond TJ, Giuvelis D, et al. In vivo characterization of MMP-2200, a mixed δ/μ opioid agonist, in mice. *J Pharmacol Exp Ther*. 2011;336:767–778.
16. Brennan TJ, Vandermeulen EP, Gebhart GF. Characterization of a rat model of incisional pain. *Pain*. 1996;64:493–501.
17. Chaplan SR, Bach F, Pogrel J, et al. Quantitative assessment of tactile allodynia in the rat paw. *J Neurosci Methods*. 1994;53:55–63.
18. Franklin KB, Paxinos G. The mouse brain in stereotaxic coordinates. Elsevier/Academic Press: Amsterdam, 2008.
19. Khroyan TV, Cipitelli A, Toll N, et al. In vitro and in vivo profile of PPL-101 and PPL-103: mixed opioid partial agonist analgesics with low abuse potential. *Front Psychiatry*. 2017;8:52.
20. Liu Y, Ji L, Eno M, et al. (R)-N-(1-Methyl-2-hydroxyethyl)-13-(S)-methyl-arachidonamide (AMG315): a novel chiral potent endocannabinoid ligand with stability to metabolizing enzymes. *J Med Chem*. 2018;61:8639–8657.
21. Selwood D. The cannabinoid receptors. Edited by Patricia H. Reggio. *ChemMedChem Chem Enabl Drug Discov*. 2009;4:1949.
22. Rinaldi-Carmona M, Barth F, Millan J, et al. SR 144528, the first potent and selective antagonist of the CB2 cannabinoid receptor. *J Pharmacol Exp Ther*. 1998;284:644–650.
23. Ross RA, Brockie HC, Stevenson LA, et al. Agonist-inverse agonist characterization at CB1 and CB2 cannabinoid receptors of L759633, L759656, and AM630. *Br J Pharmacol*. 1999;126:665–672.
24. Nikas SP, Sharma R, Paronis CA, et al. Probing the carboxyester side chain in controlled deactivation (-)-delta(8)-tetrahydrocannabinols. *J Med Chem*. 2015;58:665–681.
25. Makriyannis A. 2012 Division of medicinal chemistry award address. Trekking the cannabinoid road: a personal perspective. *J Med Chem*. 2014;57:3891–3911.
26. Zarruk JG, Fernández-López D, García-Yébenes I, et al. Cannabinoid type 2 receptor activation downregulates stroke-induced classic and alternative brain macrophage/microglial activation concomitant to neuroprotection. *Stroke*. 2012;43:211–219.
27. Whiting PF, Wolff RF, Deshpande S, et al. Cannabinoids for medical use: a systematic review and meta-analysis. *JAMA*. 2015;313:2456–2473.
28. Cottier KE, Galloway EA, Calabrese EC, et al. Loss of blood-brain barrier integrity in a KCl-induced model of episodic headache enhances CNS drug delivery. *eNeuro*. 2018;5:ENEURO.0116-18.2018.
29. Montandon G, Qin W, Liu H, et al. PreBötzing complex neurokinin-1 receptor-expressing neurons mediate opioid-induced respiratory depression. *J Neurosci*. 2011;31:1292–1301.
30. Kliewer A, Gillis A, Hill R, et al. Morphine-induced respiratory depression is independent of beta-arrestin2 signalling. *Br J Pharmacol*. 2020;177:2923–2931.
31. Breivogel CS, Wells JR, Jonas A, et al. Comparison of the neurotoxic and seizure-inducing effects of synthetic and endogenous cannabinoids with $\Delta(9)$ -tetrahydrocannabinol. *Cannabis Cannabinoid Res*. 2020;5:32–41.
32. Ossato A, Vigolo A, Trapella C, et al. JWH-018 impairs sensorimotor functions in mice. *Neuroscience*. 2015;300:174–188.
33. He Y, Galaj E, Bi GH, et al. beta-Caryophyllene, a dietary terpenoid, inhibits nicotine seeking and nicotine seeking in rodents. *Br J Pharmacol*. 2020;177:2058–2072.
34. Makriyannis A, Khanolkar A, Lu D. inventor; University of Connecticut, assignee. Cannabinoids selective for the CB2 receptor. United States 1999 September 4, 2020.
35. Ivy D, Palese F, Vozella V, et al. Cannabinoid CB2 receptors mediate the anxiolytic-like effects of monoacylglycerol lipase inhibition in a rat model of predator-induced fear. *Neuropsychopharmacology*. 2020;45:1330–1338.
36. Ludtke DD, Siteneski A, de Oliveira Galassi T, et al. High-intensity swimming exercise reduces inflammatory pain in mice by activation of the endocannabinoid system. *Scand J Med Sci Sports*. 2020;30:1369–1378.
37. Parker LA, Burton P, Sorge RE, et al. Effect of low doses of Δ 9-tetrahydrocannabinol and cannabidiol on the extinction of cocaine-induced and amphetamine-induced conditioned place preference learning in rats. *Psychopharmacology*. 2004;175:360–366.
38. Pertwee RG. Pharmacology of cannabinoid CB1 and CB2 receptors. *Pharmacol Ther*. 1997;74:129–180.
39. UNODC World Health Organization. Opioid overdose: preventing and reducing opioid overdose mortality. Vienna: United Nations Office of Drugs and Crime, World Health Organization, 2013.
40. Pfitzer T, Niederhoffer N, Szabo B. Central effects of the cannabinoid receptor agonist WIN55212-2 on respiratory and cardiovascular regulation in anaesthetised rats. *Br J Pharmacol*. 2004;142:943–952.

Cite this article as: Wiese BM, Liktör-Busa E, Levine A, Couture SA, Nikas SP, Ji L, Liu Y, Mackie K, Makriyannis A, Largent-Milnes TM, Vanderah TW (2020) Cannabinoid-2 agonism with AM2301 mitigates morphine-induced respiratory depression, *Cannabis and Cannabinoid Research* 6:5, 401–412, DOI: 10.1089/can.2020.0076.

Abbreviations Used

ANOVAs = analyses of variance
 AUC = area under the curve
 BPM = breaths per minute
 CB1R = cannabinoid-1 receptor
 CB2R = cannabinoid-2 receptor
 cDNA = complementary DNA
 CO₂ = carbon dioxide/oxygen
 CT = cycle thresholds
 ECs = endocannabinoids
 GAPDH = glyceraldehyde phosphate dehydrogenase
 IgG = immunoglobulin G
 MOR = mu opioid receptor
 mRNA = messenger RNA
 MS = morphine sulfate
 PAG = periaqueductal gray
 pBc = preBötzing complex
 qPCR = quantitative PCR
 RT-PCR = real-time PCR
 SEM = standard error of the mean
 TBST = tris-buffered saline with Tween 20
 THC = Δ^9 -tetrahydrocannabinol